Available online at www.sciencedirect.com
ScienceDirect
Journal of the European Ceramic Society 26 (2006) 3753–3759
www.elsevier.com/locate/jeurceramsoc

A study on co-firing between $Zn_{0.9}Mg_{0.1}TiO_3$ and ZnO-based multilayer varistor

W.S. Lee [a,*], W.T. Chen [a], Tony Yang [b], Y.C. Lee [b], S.P. Lin [b], C.Y. Su [a], C.L. Hu [b]

[a] *Department of Electrical Engineering, National Cheng Kung University, Taiwan*
[b] *R&D Technology Center, Yageo Corporation Nantze Branch, Taiwan*

Received 14 September 2005; received in revised form 2 December 2005; accepted 9 December 2005
Available online 2 March 2006

Abstract

A semi-conducting ZnO-based multilayer varistor (MLV) is cofired with a passivation layer with $Zn_{0.9}Mg_{0.1}TiO_3$ (ZMT) composition to prevent ZnO-based MLV from over-nickel coating during nickel plating. The cofiring results show that no de-lamination between ZMT and ZnO can be found, suggesting good co-firing compatibility between ZMT and ZnO though the anisotropic densification of ZMT is noted. However, the microstructure and electrical properties of ZnO based MLV is greatly influenced since ZMT is cofired with ZnO-based MLV. Reduction of grain size of ZnO-based MLV from 5.2 to 3.7 μm that is presumably attributed to constraining sintering of ZnO-based MLV by ZMT is observed after cofring ZMT. Simultaneously, the reduction of grain size of ZMT covered ZnO-based MLV results in a decrease of capacitance and in an increase of breakdown voltage. On the other hand, a decrease of non-linear coefficient and an increase of leakage current of ZMT covered ZnO-based MLV are observed as well. The results are associated with the change of slope of *I–V* curve for ZMT covered ZnO-based MLV due to the formation of a semi-conducting Zn_2TiO_4 phase, which is resulted from the diffusion of titanium ion into the matrix of ZnO-based MLV during co-firing.

Keywords: Constraining sintering; ZnO; Sintering; Varistor; (Zn, Mg)TiO_3

1. Introduction

Surface mountable multilayer zinc oxide varistor[1,2] have become important protection components in modern electronics for automotive, telecommunication, data processing, and consumer application because of its exceptional non-linear ohmic characteristic.

Trends in surface mount technology towards lower solder temperature, shorter time of exposure to molten solder, use of milder solder flux, and geometry restrictions on land pads lead to even small process window. As a result, there is an increasing inquiry for "nickel barrier termination" for multilayer ceramic components such as zinc oxide varistor, barium titanate capacitor. There is, however, a major hindrance for introduction of nickel barrier termination system for ZnO-based varistors that is a semi-conducting ceramic resulted of a complete coating of the multilayer ZnO varistor, when plating termination is followed barium titanate multilayer capacitor.[3]

To overcome above plating issue, the multilayer ZnO varistor covered with an insulting passivation layer is necessary. As both the ZnO-based MLV and the passivation layer of insulating ceramic undergo the same thermal treatment process, i.e. sintering, there are some aspects, which have to be considered.

1. Matching of the shrinkage behavior between two different ceramics during co-firing process.
2. The passivation layer diffuses into the electrical active zone to change ZnO-based MLV microstructure and electrical properties after co-firing.
3. The passivation layer chemically reacts with ZnO-based MLV resulting in the formation of new crystal phases.

In this study, ZnO-based MLV with B_2O_3 sintering aid addition is able be sintered from 950 °C for 1.5 h. To minimize the mismatch of sintering temperature between two ceramic materials, the sintering temperature of passivation layer should be close to the sintering temperature of ZnO-based MLV as possible. In addition, for avoidance of chemical reactions between two ceramic materials resulting in undesired crystal phases,

* Corresponding author. Tel.: +886 6 2757575; fax: +886 6 2345482.
E-mail address: leewen@mail.ncku.edu.tw (W.S. Lee).

0955-2219/$ – see front matter © 2006 Elsevier Ltd. All rights reserved.
doi:10.1016/j.jeurceramsoc.2005.12.027

the composition of passivation layer, besides it is an insulating materials sintered in air, the similarity of two ceramic materials should be as close as possible. Taking into account above two criterions, zinc titanates $ZnTiO_3$ was selected as a passivation layer in this investigation because zinc titanates ($ZnTiO_3$) can be sintered at 1100 °C without sintering aids.[7] When B_2O_3 as a sintering aid was added, the sintering temperatures of zinc titanates can be further down around 950 °C.[4,5] However, zinc titanates is a not stable phase above 820 °C, addition of Mg to stabilize zinc titanates phase formation above 820 °C is necessary according previous studies.[6] Therefore, $Zn_{0.95}Mg_{0.05}TiO_3$ (ZMT) with B_2O_3 addition is main composition as a passivation layer in this study. It is the purpose of the present study to understand what is happened after cofring ZnO-based MLV with passivation ZMT. Diffusion and chemical reaction between ZnO-based MLV and passivation ZMT would be main point we studied, as well the influence of cofiring ZnO-based MLV with passivation ZMT on the microstructure, electrical properties of ZnO-based MLV is another focus we interested in following text.

2. Experimental procedures

2.1. Preparation of multilayered varistor (MLV) covered with ZMT passivation

ZnO-based multilayered varistors (MLV) were fabricated by a conventional multi-layer ceramic capacitor (MLCC) technology. $Zn_{0.9}Mg_{0.1}TiO_3$ (ZMT) was used as the cover layer. ZnO (ZnO, Mitsui Inc., Japan) and dopants including $Al(OH)_3$, MnO, CoO, Sb_2O_3 and Bi_2O_3 were weighed, mixed, dispersed, and milled in deionized water with 2 mm yttria-tetragonal zirconia polycrystal (Y-TZP) beads for 6 h. The mean particle size (D_{50}) of milled slurry was about 0.35 μm. The pre-milling slurry were mixed with binder, and plasticizer. The resulting slip was cast into a green sheet with a 30 μm in thickness using the doctor-blade method. The Ag/Pd inner pastes were printed onto the ZnO green sheet then these printed and unprinted sheets were alternately stacked, laminated and cut into chips. Besides, ZMT green sheets were also placed on top and bottom of the ZnO MLV to study the co-firing behavior. The green chips were debinded at 320 °C and then sintered between 930 and 1000 °C for 1.5 and 2 h.

2.2. Measurements

The microstructures of the specimens were characterized by scanning electron microscope (Leo 1530, Philips Instrument Inc., Netherlands or JSM-5300, JEOL, Japan) equipped with an energy-dispersive spectrometer (EDS, EDAX Inc., USA). The thermal etching was performed at 850 °C for 20 min to reveal the grain boundary. The grain size was measured by using the linear intercept method. The co-firing of the specimen was investigated by thermo-mechanical analyzer (TMA). The specimens were heated up to 950 °C at a heating rate was 5 °C/min. The capacitance and dissipation factor ($\tan\delta$) were measured at 1 MHz by using a precision LCR network analyzer (4278A, Hewlett-Packard Inc., USA). The nonlinearity (α) was calculated from two pairs of voltage and current values and defined as $\alpha = (\log I_2 - \log I_1)/(\log V_2 - \log V_1)$. The voltage values were recorded at an applied current of 1 and 10 mA, respectively. All of the testing parameters were followed according to IEC 60060 and IEC61000-4-2.

3. Results and discussion

3.1. Shrinkage rate of sintering behavior

To understand the co-firing behavior between ZnO-based MLV and passivation ZMT materials, thermal mechanical analysis (TMA) was conduced to measure their shrinkage rate with sintering temperature. Fig. 1 demonstrates the TMA results of individual ZnO-based MLV, ZMT passivation materials and ZMT-covered ZnO-based MLV composite. The result indicates the isotropic shrinkage (curves 1 and 2) of ZnO-based MLV. The onset temperature of ZnO-based MLV is about 780 °C. The shrinkage of 32.5% either along the *X*- or *Z*-direction is observed. However, the anisotropic sintering of ZMT is noted in the *X*- and *Z*-direction (curves 5 and 6), which has an onset temperature of 830 °C. The shrinkage of 25 and 35% along the *X*- and *Z*-direction is measured, respectively. This differential densification may result in the poor dispersion of ZMT slurry and contributed to in-homogeneity of tape quality. Moreover, the shrinkage behavior of ZMT-covered ZnO MLV is illustrated in curves 3 and 4. The onset temperature of ZMT-covered ZnO-based MLV composite is 776 °C that is close to the onset

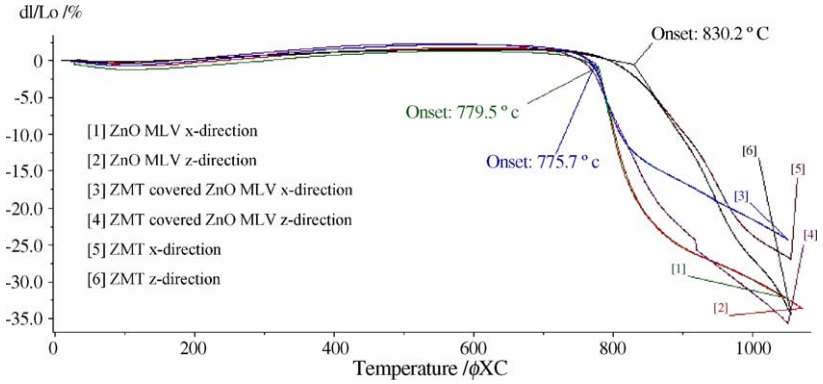

Fig. 1. TMA results of ZnO based MLV, ZMT and ZMT covered ZnO based MLV.

Table 1
TMA shrinkage behavior in *X*- and *Z*-axial for ZnO-based MLV, ZMT and ZMT covered ZnO-based MLV

	X-axial		*Z*-axial	
	Onset temperature (°C)	Shrinkage rate (%)	Onset temperature (°C)	Shrinkage rate (%)
ZnO-based MLV	780	−32.5	780	−32.5
ZMT	830	−25	830	−35
ZMT covered ZnO-based MLV	776	−28	776	−34

temperature of ZnO-based MLV, indicating the densification of ZMT-covered ZnO MLV is mainly dominated by ZnO-based MLV. The shrinkage of 28 and 34% along the *X*- and *Z*-direction is observed. Sintering behavior measured by TMA for three materials is summarized in Table 1. In comparison of ZMT, the differential densification of ZMT-covered ZnO based MLV composite can slightly decrease from 10 down to 6% due to the presence of isotropic of ZnO-based MLV.

3.2. Microstructure analysis

Fig. 2 shows the cross-sectional SEM micrograph of ZMT-covered ZnO MLV, co-fired at 950 °C/1.5 h and then thermally etched at 850 °C/20 min. The protection layer of ZMT in the range of 12 μm has an excellent bonding with ZnO matrix. No de-lamination between ZMT and ZnO can be found after the co-firing. The interfacial reaction between ZMT and ZnO is quite significant. In the inter-diffusion zone, a dual-phase microstructure is formed as shown in Fig. 3. The white phase, consisting of ZMT phases diffuses from the ZMT into ZnO and forms a continuous phase in the matrix.

To identify what new phase is formed, the element mapping for the before and after cofiring specimens were examined by SEM and XRD. ZMT consists of Mg, Zn and Ti components, the concentration difference of ZnO-based MLV before and after cofiring with ZMT are compared as shown in Fig. 3a–f. Evidently, according to mapping results, the mainly obvious difference of concentration of element is titanium after co-firing. It hints that the diffusion of Ti^{4+} into ZnO based MLV from ZMT was happened during co-firing. When X-ray diffraction meter was conducted to examine the after co-firing specimen with ZMT and ZnO-based MLV, there are two new phases formation of Zn_2TiO_4 and TiO_2 as shown in Fig. 4. According to the phase transformation reaction as below:[7]

$$2ZnO + 2TiO_2 \xrightarrow{700\,^{\circ}C} 2ZnTiO_3 \xrightarrow{950\,^{\circ}C} Zn_2TiO_4 + TiO_2$$

For the cover layer with (Zn, Mg)TiO_3 formulation, due to the presence of magnesium that is well known to suppress above decomposition reaction at 950 °C, thus, even if the specimen had been fired above 950 °C, above phase transformation reaction at 950 °C was not able to be occurred. The main phase of the cover layer is still kept (Zn, Mg)TiO_3. However, on the contrary, when co-firing between (Zn, Mg)TiO_3 with ZnO based MLV, only titanium ion from ZMT was diffused into ZnO based MLV, in other words, no diffusion of Mg^{2+} into ZnO-based MLV was observed. It hints that the decomposition reaction of $2ZnTiO_3$ into $Zn_2TiO_4 + TiO_2$ two phases would be occurred due to the lack of suppressor such as magnesium.[8]

A typical grain size distribution of the specimens of ZnO-based MLV, sintered at 950 °C/1.5 h is shown in Fig. 5a and b. The average grain of the specimen is about 5.2 μm. However, the distribution of grain size is quite large, probably due to the liquid phase sintering in the presence of Bi_2O_3. The grain size can be as

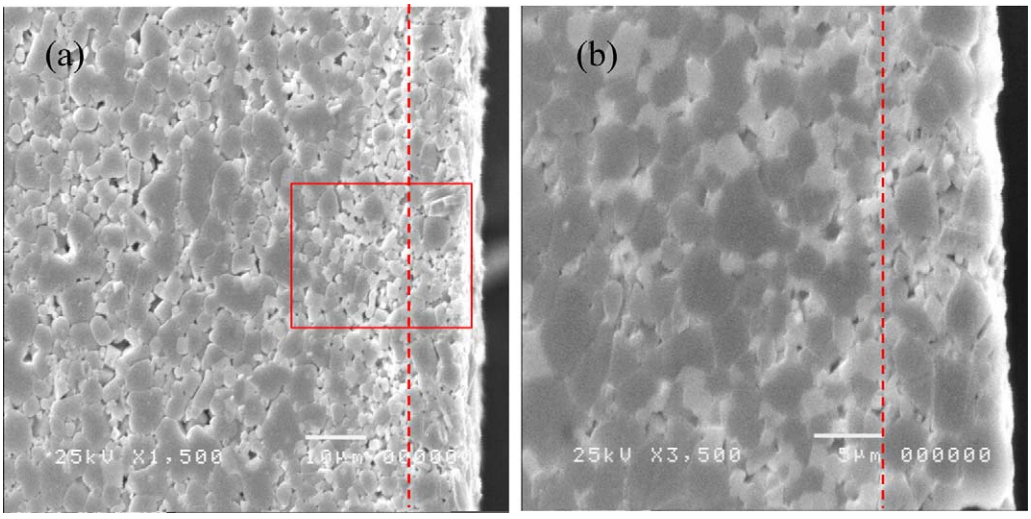

Fig. 2. (a and b) SEM micrographs of co-fired ZMT-ZnO-based MLV at 950 °C for 1.5 h. The specimen was thermally etched at 850 °C for 20 min.

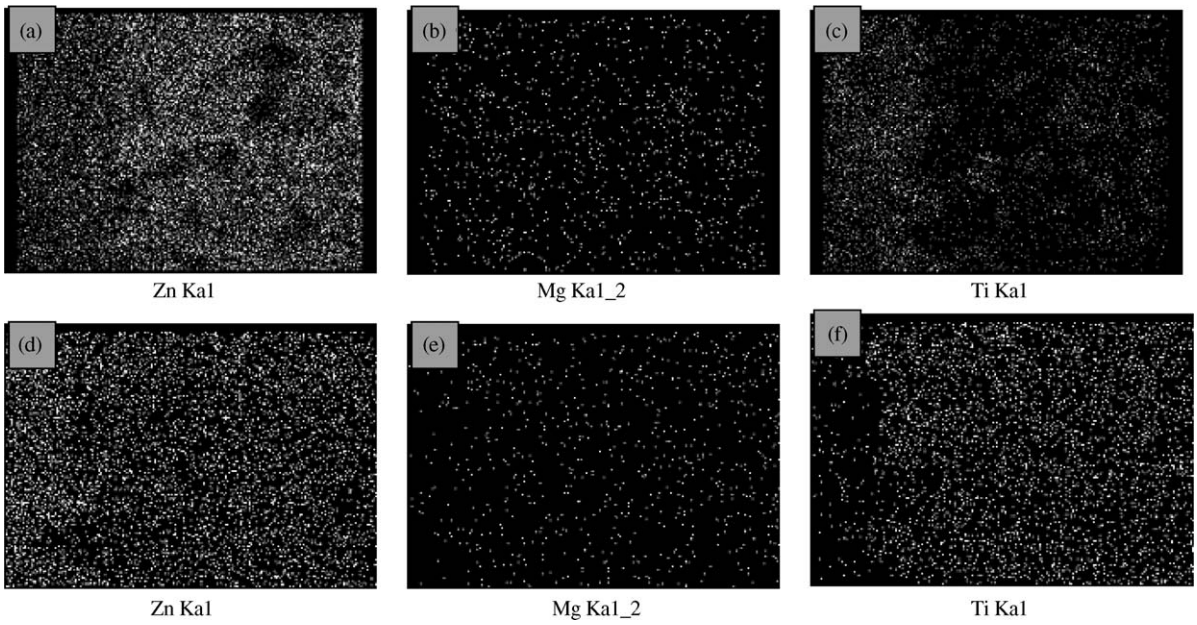

Fig. 3. (a–c) Micrographs of Zn, Mg, Ti mapping before co-firing between ZMT and ZnO-based MLV at 950 °C for 1.5 h. (d–f) Micrographs of Zn, Mg, Ti mapping after co-firing between ZMT and ZnO-based MLV at 950 °C for 1.5 h.

small as 2.0 μm and as big as 12.0 μm. An improvement in the grain size distribution will be needed to obtain a more uniform microstructure.

Fig. 6a and b show the SEM micrograph of ZMT-covered ZnO-based MLV, which was thermally de-binded at 350 °C. More importantly, the grain size of ZnO-based matrix is greatly reduced to 3.7 μm while ZnO based MLV co-firing with cover-layer of ZMT.

There are two possible causes to explain for why the grain size of ZnO based MLV is greatly decreased while co-firing with the cover layer of ZMT. One is the most possible speculation is that the grain growth of ZnO-based MLV is constrained by the cover-layer of ZMT during co-firing due to the mismatch of onset sintering temperature between them.[9] As mentioned in the previous section, the onset sintering temperature for ZnO-based MLV is lower than that of ZMT. When co-firing temperature approaches 780 °C, the ZnO based MLV will start to shrink, however, the cover-layer of ZMT is still kept non-shrinkage due to its high onset sintering temperature. Thus, the shrinkage of ZnO-based MLV would be constrained by the cover-layer of ZMT in the direction of x and y directions, resulting in the inhibition of grain growth for ZnO based MLV.[10] Another possible

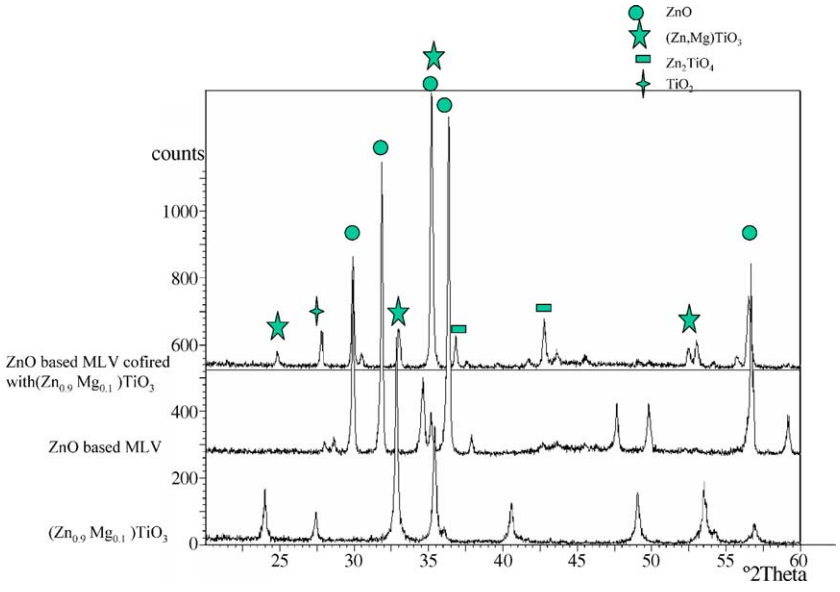

Fig. 4. XRD pattern for ZMT, ZnO based MLV and ZnO based MLV cofired with ZMT.

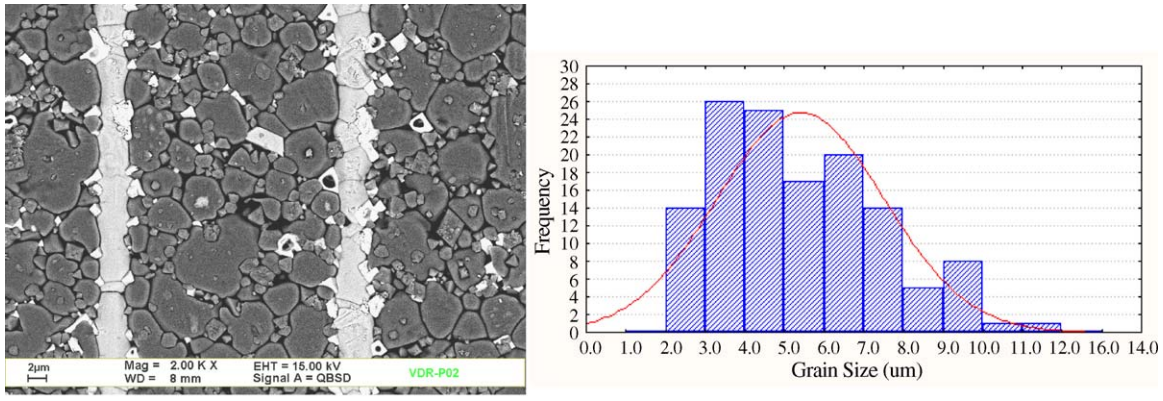

Fig. 5. (a and b) SEM micrograph and grain size distribution of ZnO-based MLV sintered at 950 °C for 1.5 h.

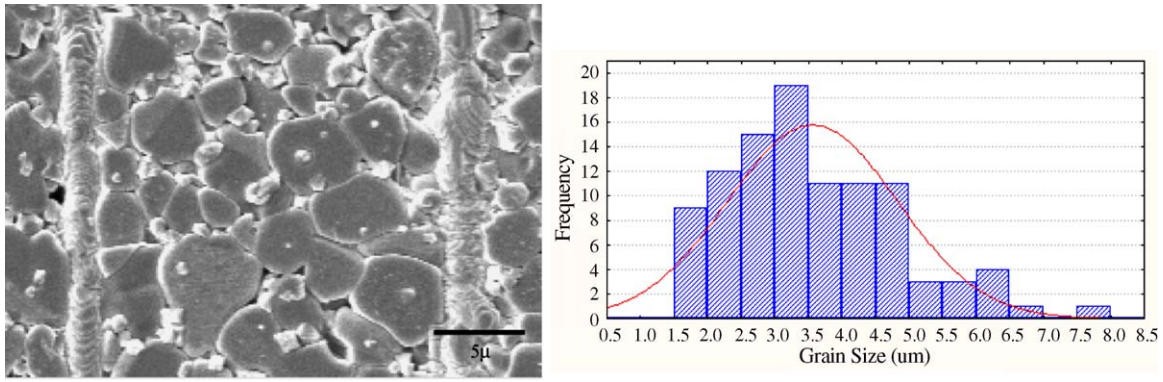

Fig. 6. (a and b) SEM micrograph and grain size distribution of ZMT covered ZnO-based MLV sintered at 950 °C for 1.5 h.

reason is suspected when Ti^{4+} was diffused from the cover-layer of ZMT into ZnO based MLV and two new phases (Zn_2TiO_4, TiO_2) were formed that hamper the grain growth of ZnO-based MLV. Though previous investigations had demonstrated that Ti^{4+} addition into ZnO plays a accelerator of grain growth of ZnO matrix,[11] however, in our study, Fig. 3f shows large amount of Ti^{4+} was diffused into ZnO-based MLV matrix resulting a few of the second phases were formed and widely distributed in ZnO-based MLV matrix. The role of the second phase in inhibition of grain growth of ZnO-based MLV is taken into account.

3.3. Electrical properties analysis

Table 2 summarizes the electrical properties of ZnO based MLV and ZMT-covered ZnO based MLV, co-fired at 950 °C/1.5 h. The results show that the application of ZMT on top and bottom as a cover layer leads to a decrease in capacitance and an increase in breakdown voltage. Capacitance is strongly decreased from 90nF to 35pF, on the other hand, the breakdown voltage is enhanced from 8.8 to 13.8 V. Both of effects are presumably attributed to the reduction of grain size.

Table 2
Electrical properties of ZnO based MLV and ZMT covered ZnO-based MLV, sintered at 950 °C for 1.5 h

	Capacitance (pF)	V_B (V)	α-value	Leakage current (A)
ZnO-based MLV	90	8.8	18.8	0.04
ZMT covered ZnO-based MLV	35	13.8	12.5	0.2

It is well known that the ZnO-based varistor possesses the characteristic of grain boundary capacitors. The effective dielectric constant can be expressed as[12]:

$$\varepsilon_{\text{eff}} = \varepsilon_{\text{i}} \frac{d_{\text{g}}}{d_{\text{i}}} \quad (1)$$

where $\varepsilon_{\text{i}}, d_{\text{g}}, d_{\text{i}}$ represent dielectric constant of insulating layer at grain boundary, grain size of matrix and thickness of insulating phase at grain boundary, respectively. The effective dielectric constant of ZnO-based MLV is directly proportional to the dielectric constant of insulting phase (ε_{i}), and grain size of the matrix (d_{g}) but reversely proportional to the thickness of insulting phase (d_{i}). As ε_{i} is almost a constant and d_{i} is quite small, d_{g} may play an important role in determining the capacitance of ZMT-covered ZnO MLV.

Usually, a small grain size will lead to a big breakdown V_B of ZnO based MLV.[13] The individual breakdown voltages of all grain boundaries, which form the current path between the external electrodes, add up to the total breakdown voltage of the

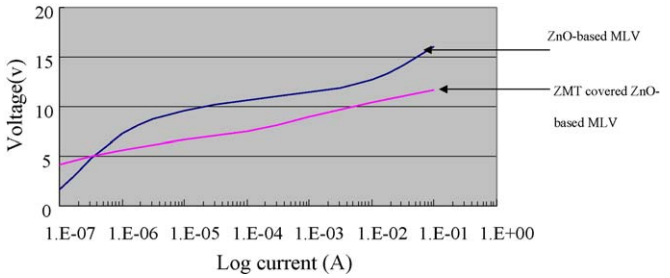

Fig. 7. *I–V* curve for ZMT, ZnO based MLV and ZMT covered ZnO based MLV.

ZnO-based multilayer varistor following the formula (2).

$$V = N_{GB} \times V_{GB} = \left(\frac{L}{d_g}\right) \times V_{GB} \quad (2)$$

Where N_{GB} is the number of grain boundaries N_{GB}, V_{GB} is the breakdown voltage per grain boundary, L is the thickness between two electrodes, and d_g is the diameter of average grain size. Obviously, the breakdown voltage of ZnO-based MLV can be well controlled by either changing the grain size or changing the thickness between two electrodes.[14] For ZnO based MLV specimen, the breakdown voltage (V) is 8.8 V, the thickness of two electrodes (L) is 20 μm and the average grain size(d_g) is 5.8 μm. As a result, calculation of the breakdown voltage per grain (V_{GB}) is 2.55 V. On the other hand, for ZMT covered ZnO-based MLV specimen, the breakdown voltage (V) is 13.8 V, the thickness of two electrodes (L) is 20 um and the average grains size (d_g) is 3.7 um, based on these parameters, calculation of the breakdown voltage per grain (V_{GB}) is 2.55 V, too. It is interested to note that the breakdown voltage per gain is the same for ZnO based MLV and ZMT covered ZnO based MLV.

While ZMT was co-fired with ZnO based MLV, an increase in leakage current from 0.04 to 0.2 μA and a decrease in non-linear coefficient from 18.8 to 12.5 are both observed. This result is associated with the formation of a semi-conducing Zn_2TiO_4 resulting in changing *I–V* curve behavior for ZMT covered ZnO-based MLV. Fig. 7 shows the current-voltage curve for ZnO-based MLV and ZMT covered ZnO based MLV. A significant difference of *I–V* curves between them is observed maybe due to the present of semi-conducting phase of Zn_2TiO_4. In general, there are three regions in *I–V* curve of varistors. The leakage current of ZnO-based MLV is mainly determined by the slope of *I–V* curve slope in the leakage current region of ZnO-based MLV. Evidently, the slope of ZMT covered ZnO-based MLV is smaller than that of ZnO-based MLV. It indicates that leakage current is increased when the semi-conducting phase of Zn_2TiO_4 is existed. On the other hand, the non-linear coefficient of ZnO-based MLV is determined by the slope of *I–V* in the normal operating region. It is obvious to see the slope of ZMT covered ZnO-based MLV is bigger than that of ZnO-based MLV, corresponding to the non-linear coefficient of ZMT covered ZnO-based MLV is smaller than of that of ZnO-based MLV. This result is still associated with the presence of semi-conducting phase of Zn_2TiO_4 leading to a change of the slope of *I–V* curve.[15]

4. Conclusion

The anisotropic densification of ZMT is noted while the isotropic shrinkage of ZnO is observed. The differential densification of ZMT-covered ZnO MLV leads to no de-lamination of ZMT from ZnO matrix. The application of $Zn_{0.9}Mg_{0.1}TiO_3$ZMT as a cover passivation layer on top and bottom of ZnO MLV is successfully co-fired with ZnO-based MLV for improvement on resistance to acidic plating.

In comparison with ZnO-based MLV, the average and distribution of grain size for ZnO-based MLV coifirng with $Zn_{0.9}Mg_{0.1}TiO_3$ are both reduced, indicating the homogeneity of microstructure is greatly improved. The grain growth of ZnO-based MLV are probably constrained by the presence of $Zn_{0.9}Mg_{0.1}TiO_3$ cover layer or probably inhibited by the formation of Zn_2TiO_4 phase distributed in ZnO-based MLV matrix due to the diffusion of titanium during cofiring.

ZnO based MLV as cofired with $Zn_{0.9}Mg_{0.1}TiO_3$ cover layer results in a decrease in capacitance and an increase in breakdown voltage mainly due to the reduction of grain size. On the other hand, a decrease in non-linear coefficient and an increase in leakage current is associated with the change of slope of *I–V* curve for ZMT covered ZnO-based MLV due to the formation of semi-conducting Zn_2TiO_4 phase.

Acknowledgement

The authors would like to acknowledge the financial support under contract No. NSC94-2213-E006-048.

References

1. Levinson, L. M. and Philipp, H. R., Zinc oxide varistor–a review. *Ceram. Bull.*, 1986, **65**(4), 639–646.
2. Gupta, T. K., Application of zinc oxide varistors. *J. Am. Ceram. Soc.*, 1990, **73**(7), 1817–1840.
3. Shohata, N., Nakanishi, M. and Utsumi, K., Multilayer ceramic chip varistor. In *Ceramic transaction*, *vol. 3: Advances in varistor technology*, ed. L. M. Levinson. Am. Ceram. Soc, Westerville, OH, 1989.
4. Kim, H. T., Byun, J. D. and Kim, Y., Microstructure and microwave dielectric properties of modified zinc titanates (I). *Mater. Res. Bull.*, 1998, **33**(6), 963–973.
5. Kim, H. T., Kim, S. H., Nahm, S. and Byun, J. D., Low-temperature sintering and microwave dielectric properties of zinc metatitanate-rutile mixtures using boron. *J. Am. Ceram. Soc.*, 1999, **82**(11), 3043–3048.
6. Kim, H. T., Nahm, S. and Byun, J. D., Low-fired (Zn, Mg)TiO_3 microwave dielectrics. *J. Am. Ceram. Soc.*, 1999, **82**(12), 3476–3480.
7. Kim, H. T., Byun, J. D. and Kim, Y., Microstructure and microwave dielectrical properties of modified zinc titanates (II). *Mater. Res. Bull.*, 1998, **33**(6), 975–986.
8. Sugiura, M. and Ikeda, K., Studies on dielectrics of TiO_2–ZnO system. *J. Jpn. Ceram. Assoc.*, 1947, **55**(626), 62–66.
9. Lin, Y. C. and Jean, J. H., Constrained densification kinetics of alumina/borosilicate glass + alumina/alumina sandwich structure. *J. Am. Ceram. Soc.*, 2002, **85**(1), 150–154.
10. Hsu, R. T. and Jean, J. H., Key factors controlling camber behavior during the cofiring of bi-layer ceramic dielectric laminate. *J. Am. Ceram. Soc.*, 2005, **88**(9), 2429–2434.
11. Homma, T. and Yamaguchi, T., Reaction of multiphase ceramics-system ($Zn_2TiO_4 + TiO_2$)-ZnO and $CaCO_3$. *J. Ceram. Soc. Jpn.*, 1997, **105–771**.

12. Goodman, G., Capacitors based on ceramic grain boundary barrier layers: a review. In *Grain boundary phenomena in electronic ceramics*, *vol. 1: Advances in ceramics*, ed. L. M. Levinson and D. C. Hill. Am. Ceram. Soc, Columbus, OH, 1981, p. 215.
13. Hennings, D. F. K., Hartung, R. and Reijnen, P. J. L., Grain size control in low voltage varistor. *J. Am. Ceram. Soc.*, 1990, **73**(3), 645–648.
14. Bowen, L. J. and Avella, F. J., Microstructure, electrical properties, and failure prediction in low clamping voltage zinc oxide varistors. *J. Appl. Phys.*, May 1983, **54**(5).
15. Carlson, W. G. and Gupta, T. K., Improved varistor nonlinear via donor impurity doping. *J. Appl. Phys.*, Aug 1982, **53**(8).